

Digit anomalies in the hadronic mass spectrum, Shannon information entropy, and the dynamical QCD scale

R. da Rocha  ^{1,*} and R. D. Vilela  ^{1,†}

¹*Federal University of ABC, Center of Mathematics,
Santo André, São Paulo 09580-210, Brazil*

Quantum Chromodynamics (QCD) has an emergent dynamical energy scale Λ_{QCD} which sets the threshold between perturbative and nonperturbative regimes. This characteristic scale causes hadronic masses to cluster within certain mass ranges, instead of following a uniform distribution. Analyzing the Shannon information entropy underlying the hadronic mass spectrum provides novel insight into this phenomenon, revealing a pronounced deviation from the law of anomalous numbers. This deviation quantifies the emergence of the dynamical scale in strongly interacting systems, also encoding the information-entropy cost associated with the breaking of scale invariance in QCD.

I. INTRODUCTION

Shannon's seminal paper [1] forged information into a quantitative concept that underlies communication theory, establishing the foundation for error-correcting codes and data-compression algorithms. Shannon information entropy categorizes the evolution of dynamical systems among regular, chaotic, and completely random regimes, making it particularly useful in nuclear reactions [2–4]. The production of hadrons in heavy-ion collisions is difficult to analyze directly, owing to the intricate and rapidly evolving dynamics of nuclear matter. Applications of Shannon information entropy include the analysis of chaotic patterns in hadron branching processes and in the quark-gluon plasma (QGP), a short-lived, thermalized QCD phase of deconfined, ultra-dense hot nuclear matter. Shannon information entropy comprises the fundamental quantity in configurational information measures (CIMs) [5–8], which have been explored to address physical aspects of hadronic matter in QCD. The hadronic mass spectrum have been comprehensively

*Electronic address: roldao.rocha@ufabc.edu.br

†Electronic address: rafael.vilela@ufabc.edu.br

investigated using CIMs to estimate the mass spectrum of heavier resonances in several meson and baryon families [9–20], supporting experimental data reported in the Particle Data Group (PDG) [21]. One can also delve into several relevant aspects and applications of quantum field theory using Shannon information entropy [22–26].

The distribution of the full widths of hadrons was shown to satisfy the law of anomalous numbers [27], also known as Newcomb–Benford’s law [28], which was also employed to scrutinize nuclear structure physics [29]. This law asserts that the leading digits of certain naturally occurring datasets follow a logarithmic distribution in which smaller digits appear more frequently. Similar patterns arise in analyzing pulsars [30], gamma-ray bursts [31], scaling phenomena [32], and fermionic/bosonic distributions in statistical mechanics [33].

The main objective of this work is to apply the Shannon information entropy to the distribution of the hadronic mass spectrum in QCD and to show that the leading digit in hadron masses violates Newcomb–Benford’s law, which maximizes Shannon information entropy if scale invariance is assumed. The departure from the Newcomb–Benford’s law arises from the existence of a fundamental scale, Λ_{QCD} , that breaks scale invariance. It selects preferred hadronic mass ranges, thereby creating hadron mass clusters, ranging from 139 MeV to 11.1 GeV. This feature is supported by the Hagedorn pattern¹ of the density of states [34]. The leading-digit distribution of the hadronic mass spectrum will be shown in this work to have lower Shannon information entropy, as compared to the Newcomb–Benford probability distribution. This offset quantifies the extent to which QCD breaks scale invariance: while the Newcomb–Benford distribution corresponds to the maximal Shannon information entropy of a scale-invariant system, the hadronic mass spectrum displays a Shannon information entropy deficit that encodes how QCD dynamics impose a preferred energy scale on the hadronic mass spectrum landscape.

This paper is organized as follows: Section II introduces the fundamental aspects of Shannon information entropy and shows that, under the assumption of scale invariance, it is maximized by the Newcomb–Benford probability distribution. Section III analyzes Shannon information entropy associated with the leading-digit distribution of the hadronic mass spectrum as listed in PDG [21], showing the breakdown of Newcomb–Benford’s law due to the scale Λ_{QCD} . This is accomplished by comparing the Shannon in-

¹ In Appendix B, the Hagedorn growth, associated with QCD ultraviolet spectrum, and the mass gap intrinsic to infrared confinement, will be presented as dual manifestations of the existence of Λ_{QCD} .

formation entropy deficit between the observed hadron spectrum and Newcomb–Benford expected probability distribution. The analysis is split into three cases: (i) mesons, (ii) baryons, and (iii) the combined meson-baryon dataset. Appendices A and B provide detailed derivations: the variational proof of Newcomb–Benford’s law as a maximum Shannon information entropy distribution; scale symmetry breaking in QCD, and an overview of hadronic mass clustering and the Hagedorn spectrum arising from counting the number of hadronic density of states, and the mass gap.

II. SHANNON INFORMATION ENTROPY UNDER SCALE INVARIANCE AND QCD SCALE INVARIANCE BREAKING

Information communication protocols aim to reproduce a selected message through a channel. For an ordered system with discrete events $H = \{E_1, E_2, \dots, E_n\}$, respectively with probabilities $P = \{p_1, p_2, \dots, p_n\}$, Shannon defined the information entropy of the message space as

$$S = - \sum_{i=1}^n p_i \ln p_i, \quad \sum_{i=1}^n p_i = 1, \quad (1)$$

measuring the number of bits to which a message with n events can be compressed [8]. If all events are equally probable ($p_i = 1/n$), the Shannon information entropy reduces to $S = \ln n$, whereas selecting among a single possible event carries no uncertainty and yields $S = 0$. With the base- e logarithm, Shannon information entropy is expressed in the natural unit of entropy (nat), corresponding to the information associated with an event occurring with probability e^{-1} .

We aim to calculate and analyze the Shannon information entropy for the leading-digit distribution of the hadronic mass spectrum. First, under the assumption of scale invariance, the Newcomb–Benford distribution will be shown to be the only probability density that maximizes Shannon information entropy. To be as general as possible, this demonstration will be implemented for the differential Shannon information entropy². For a continuous probability distribution $P(x)$ defined on \mathbb{R}^+ , Shannon information entropy takes the form

$$S[P] = - \int_0^\infty P(x) \ln P(x) dx. \quad (2)$$

Eq. (2) defines the (differential) Shannon information entropy, which can be thought of

² The demonstration of the discrete case is quite a direct consequence that follows *mutatis mutandis*.

as being the continuous limit of Shannon information entropy as long as the information dimension – measuring how the information entropy increases as the measurement resolution improves – is controlled [5–8]. One can determine $P(x)$ that maximizes $S[P]$ under the assumption of scale invariance. Under scaling transformations $x \mapsto \lambda x$, for $\lambda \in \mathbb{R}^+$, scale invariance means that $P(\lambda x)d(\lambda x) = P(x)dx$, implying that $P(x)$ is a homogeneous function of degree minus one, namely $P(\lambda x) = \frac{1}{\lambda}P(x)$, whose only nontrivial solution is given by

$$P(x) = \frac{C}{x}, \quad C \in \mathbb{R}. \quad (3)$$

One can also define $y = \ln x$, introducing the probability distribution in y -space as $Q(y)dy = P(x)dx$, in such a way that

$$P(x) = \frac{Q(\ln x)}{x}. \quad (4)$$

Normalization $\int_0^\infty P(x)dx = \int_{-\infty}^\infty Q(y)dy = 1$ is assumed.

Shannon information entropy in logarithmic variables can be read off, as substituting Eq. (4) into Eq. (2) gives (introducing a cutoff for the integrand to be normalizable³)

$$S = - \int_{y_{\text{MIN}}}^{y_{\text{MAX}}} Q(y) \ln Q(y) dy + \int_{y_{\text{MIN}}}^{y_{\text{MAX}}} yQ(y) dy, \quad (5)$$

with $y_{\text{MIN}} = \ln x_{\text{MIN}}$, and $y_{\text{MAX}} = \ln x_{\text{MAX}}$. The leading term on the right-hand side of Eq. (5) is Shannon information entropy in log-space, measuring the spread over scales. Scale invariance $x \mapsto \lambda x$ for the probability distribution $P(x)$ becomes translation invariance $Q(y + \ln \lambda) = Q(y)$, whose only normalized solution is given by

$$Q(y) = \text{constant} = \frac{1}{y_{\text{MAX}} - y_{\text{MIN}}}, \quad (6)$$

which is uniform in log-space, meaning that every logarithmic scale represented by a decade is equally likely.

One can now use the probability distribution (4) which, by virtue Eq. (6), reads:

$$P(x) = \frac{1}{x(y_{\text{MAX}} - y_{\text{MIN}})} = \frac{1}{x \ln(x_{\text{MAX}}/x_{\text{MIN}})}, \quad x \in [x_{\text{MIN}}, x_{\text{MAX}}], \quad (7)$$

³ Without a finite support, Shannon information entropy maximization becomes ill-defined. The distribution $P(x) \propto \frac{1}{x}$, with $x \in (0, \infty)$, cannot be normalized, since the integral $\int_0^\infty \frac{dx}{x}$ diverges. Moreover, the left-hand side of Eq. (2) can be made arbitrarily large by spreading the probability distribution over arbitrarily wider ranges. Hence, the maximization problem demands a finite cutoff, $x \in [x_{\text{MIN}}, x_{\text{MAX}}]$, within which the maximum-Shannon information entropy solution consistent with scale invariance will be given by Eq. (7).

which is also known as the Jeffreys prior in Bayesian statistics. Under the assumption of scale invariance, Eq. (7) is the only probability distribution that maximizes Shannon information entropy. The complete formal proof is provided in Appendix A. On a compact log-interval $[y_{\text{MIN}}, y_{\text{MAX}}]$, maximizing Shannon information entropy yields a uniform density in the y variable, as

$$S[Q] = - \int_{y_{\text{MIN}}}^{y_{\text{MAX}}} Q(y) \ln Q(y) dy = \ln(y_{\text{MAX}} - y_{\text{MIN}}), \quad (8)$$

which is invariant under the shifting by $\ln \lambda$.

Now, any nonzero real number can be written as $x = m \times 10^k$, for $m \in [1, 10)$. The probability density for the mantissa m follows from integrating $P(x)$ over all decades, $P(m) \propto \int P(m \times 10^k) 10^k dk$. Since $P(x) \propto 1/x$ as given by Eq. (7), this expression becomes scale independent, and normalization yields $P(m) = \frac{1}{m \ln 10}$. The probability that the leading digit d attains any value in the set $\{1, 2, \dots, 9\}$ reads

$$P(d) = \int_d^{d+1} \frac{1}{m \ln 10} dm = \log_{10} \left(1 + \frac{1}{d} \right), \quad (9)$$

encoding the Newcomb–Benford’s law when projected onto the leading significant digit. Among all possible distributions $P(x)$ on a positive, scale-invariant domain, expression (9) – and only it – maximizes Shannon information entropy.

Consequently, under the assumption of scale invariance, the Shannon information entropy is maximized by the log-uniform Newcomb–Benford distribution, which represents the most unbiased probability density. Scale-invariant distributions describe physical systems with no preferred length or energy scale. In quantum field theory (QFT), scale invariance under renormalization group (RG) flow implies that observables exhibit the same behavior across energy scales, with no distinguished scale [35, 36]. Although classical QCD with massless quarks is scale invariant, quantum corrections break this symmetry through the running of the strong coupling, which depends on the renormalization scale μ . This introduces the characteristic dimensionful parameter of the theory, the QCD scale $\Lambda_{\text{QCD}} \sim 200\text{--}300$ MeV. For $\mu \gg \Lambda_{\text{QCD}}$, the theory lies in its perturbative regime, where the running coupling generates asymptotic freedom and quarks and gluons interact weakly. On the other hand, the energy range $\mu \lesssim \Lambda_{\text{QCD}}$ defines the nonperturbative domain and the coupling becomes strong, giving rise to confinement at low energies [37, 38], manifested in the internal structure of hadrons [39]. Further details are provided in Appendix B.

Confinement and chiral symmetry breaking generate discrete hadronic mass spectra centered between 140 MeV and 11.1 GeV. If the leading-digit distribution of hadronic masses were related to a scale-free ensemble without a preferred energy scale, Shannon information entropy would be maximized by the Newcomb–Benford statistics. In contrast, QCD dynamics introduce strong correlations and a preferred scale, as hadronization occurs near Λ_{QCD} [40, 41]. This emergent scale reduces Shannon information entropy relative to a purely scale-invariant ensemble, producing an information entropy deficit. Also, as it will be shown in Section III, it causes the leading-digit distribution of hadron masses to deviate from Newcomb–Benford’s probability distribution, thus signaling the dynamical scale in QCD. We will show that the Shannon information entropy of the hadronic mass spectrum reported by the PDG [21] deviates from the maximal (scale-invariant) value, reflecting quantum corrections in QCD that break scale invariance in the infrared regime.

III. SHANNON INFORMATION ENTROPY FOR HADRONS

Our analysis is organized into three cases, in which the Shannon information entropy of the leading-digit distribution of the hadronic mass spectrum is computed and compared with the Shannon information entropy associated with the Newcomb–Benford law. As will be shown, the latter is statistically suppressed owing to the presence of a preferred energy scale in QCD. Subsec. III A examines the meson states listed in the PDG, Subsec. III B treats the baryon sector, and Subsec. III C considers the combined meson–baryon spectrum [21]. For definiteness, let the leading digit of a hadron mass be d , with \mathcal{O}_d denoting the number of observed occurrences and $P_{\text{OBS}}(d) = \mathcal{O}_d/N$ the corresponding empirical probability, where N denotes the total number in the hadronic sample. The expected count under the Newcomb–Benford law is $\mathcal{E}_d = N P_{\text{BENF}}(d)$, where $P_{\text{BENF}}(d)$ is the associated theoretical probability distribution. The mass spectra of mesons and baryons are presented combined (Fig. 1) and separately (Fig. 2).

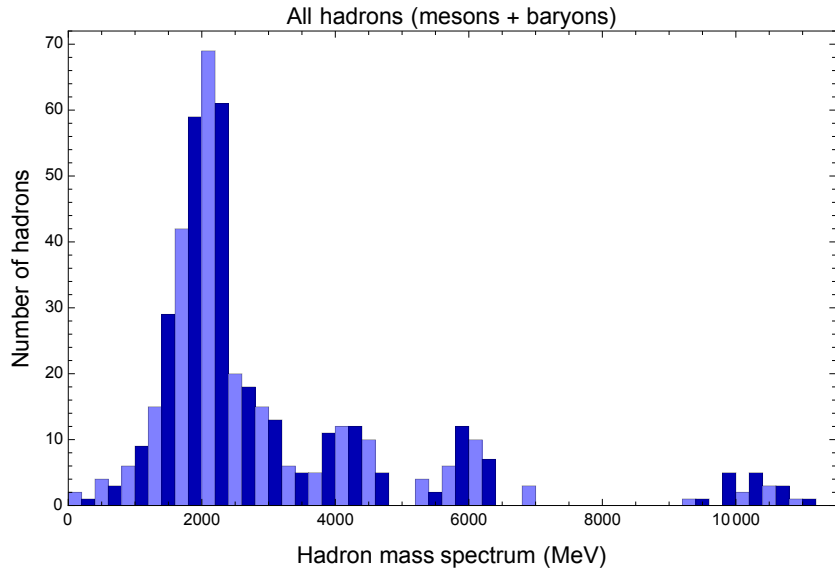


FIG. 1 Distribution of hadronic mass spectrum in PDG [21].

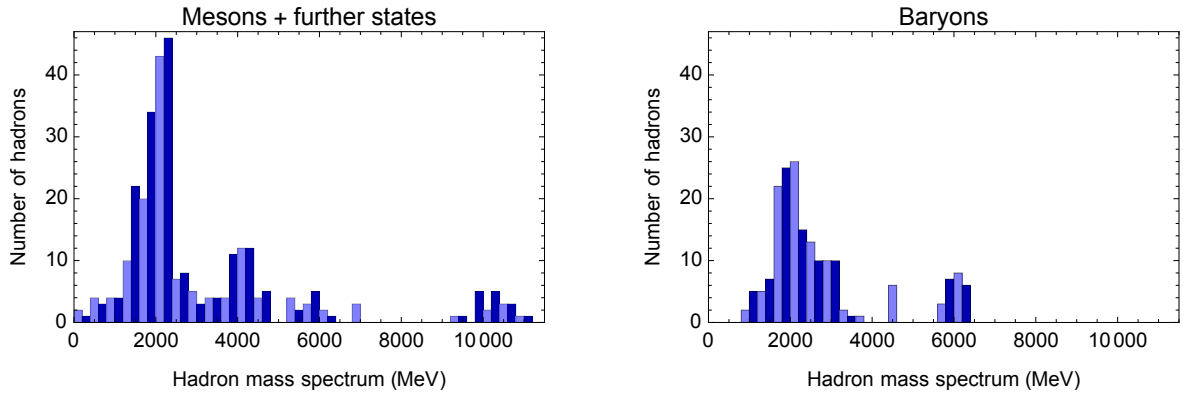


FIG. 2 Distribution of meson (with further mesonic states) [left panel] and baryon [right panel] mass spectrum in PDG [21].

A. Shannon information entropy for mesons and further mesonic states in PDG

We analyze the distribution of the meson mass spectrum, as listed in the PDG [21], whose leading digit counts are displayed in Table I.

Digit (d)	Observed (\mathcal{O}_d)	$P_{\text{OBS}}(d)$	Benford (\mathcal{E}_d)	$P_{\text{BENF}}(d)$
1	112	0.333	78.0	0.301
2	123	0.366	45.6	0.176
3	30	0.089	32.4	0.125
4	35	0.104	25.1	0.097
5	16	0.048	20.5	0.079
6	6	0.018	17.4	0.067
7	3	0.009	15.0	0.058
8	1	0.003	13.2	0.051
9	10	0.030	11.9	0.046

TABLE I Comparison of the leading-digit distribution of the meson mass spectrum (with further mesonic states) in PDG to Newcomb–Benford’s probability distribution ($N = 336$).

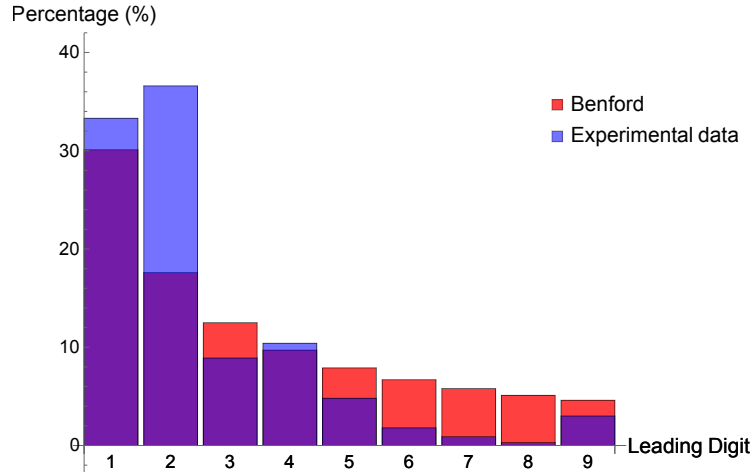


FIG. 3 Distribution of the meson mass spectrum with further mesonic states in PDG [21], according to the leading digit.

Shannon information entropy of the observed meson mass spectrum can be calculated by taking the dataset at the third column of Table I, reading

$$S_{\text{PDG}} = - \sum_{d=1}^9 P_{\text{OBS}}(d) \ln P_{\text{OBS}}(d) \approx 1.569 \text{ nat.} \quad (10)$$

The Shannon information entropy for the Newcomb–Benford distribution can be com-

puted when addressing the dataset at the fifth column of Table I, yielding

$$S_{\text{BENF}} = - \sum_{d=1}^9 P_{\text{BENF}}(d) \ln P_{\text{BENF}}(d) \approx 1.996 \text{ nat.} \quad (11)$$

The Shannon information entropy deficit reads

$$\Delta S = S_{\text{BENF}} - S_{\text{OBS}} \approx 0.427 \text{ nat,} \quad (12)$$

corresponding to a 21.37% Shannon information entropy deficit, identifying the information entropy cost of the emergence of Λ_{QCD} , indicating the deviation from scale invariance in QCD. This supports the breakdown of Newcomb–Benford’s law due to the existence of a preferred energy scale in QCD.

To quantify the deviation from Newcomb–Benford’s law, a χ^2 test can be implemented from the meson mass spectrum dataset in Table I, as

$$\chi_{\text{OBS}}^2 = \sum_{d=1}^9 \frac{(\mathcal{O}_d - \mathcal{E}_d)^2}{\mathcal{E}_d} = \sum_{d=1}^9 \frac{(NP_{\text{OBS}} - NP_{\text{BENF}})^2}{NP_{\text{BENF}}} = 179.859, \quad (13)$$

whose p -value at the 5% significance level reads

$$p = \frac{\Gamma(4, \chi_{\text{OBS}}^2/2)}{\Gamma(4)}, \quad (14)$$

where $\Gamma(s)$ is the gamma function, and $\Gamma(s, x) = \int_x^\infty t^{s-1} e^{-t} dt$ is the upper incomplete gamma function. Eq. (14) corresponds to the probability of observing a χ^2 distribution value as large or larger than the observed one under the null hypothesis – that the leading-digit distribution follows Newcomb–Benford’s law – reads $p = P(\chi^2 \geq 179.859) = 1.075 \times 10^{-34}$, which is extremely small, indicating a significant deviation from the Newcomb–Benford distribution. It supports QCD-induced energy scale effects and clustering in the meson mass spectrum. The emergence of Λ_{QCD} breaks scale invariance and lowers Shannon information entropy relative to a scale-free ensemble. Therefore, the leading-digit distribution of the meson mass spectrum and its Shannon information entropy reflect the existence of an energy scale in QCD. The Shannon information entropy deficit measures the information entropy cost of emergence of scale in QCD.

B. Shannon information entropy for baryons in PDG

The leading-digit statistics of the baryon mass spectrum can be analogously analyzed, also showing scale invariance breaking in the baryonic sector. As also holds for mesons,

if scale invariance held, the leading-digit distribution of the baryonic masses would follow Newcomb–Benford’s law. Deviations from it, therefore, quantify the degree to which QCD dynamics and confinement effects introduce preferred mass scales into the baryon spectrum. The observed and expected probabilities for each leading digit are summarized in Table II.

Digit (d)	Observed (\mathcal{O}_d)	$P_{\text{OBS}}(d)$	Benford (\mathcal{E}_d)	$P_{\text{BENF}}(d)$
1	64	0.339	45.5	0.301
2	74	0.392	26.6	0.176
3	15	0.079	18.9	0.125
4	6	0.032	14.6	0.097
5	10	0.053	11.9	0.079
6	18	0.095	10.1	0.067
7	0	0.000	8.8	0.058
8	0	0.000	7.7	0.051
9	2	0.011	6.9	0.046

TABLE II Comparison of the leading-digit distribution of baryon mass spectrum in PDG with the Newcomb–Benford’s probability distribution ($N = 189$).

Fig. 4 illustrates the observed baryon mass spectrum.

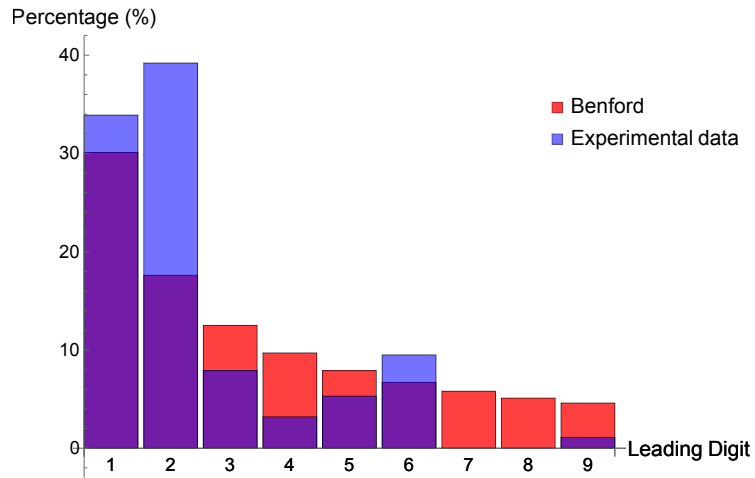


FIG. 4 Distribution of the baryon mass spectrum in PDG [21], according to the leading digit.

Shannon information entropy of the observed meson mass spectrum can be calculated

by taking the dataset at the third column of Table II, reading

$$S_{\text{PDG}} = - \sum_{d=1}^9 P_{\text{OBS}}(d) \ln P_{\text{OBS}}(d) \approx 1.472 \text{ nat.} \quad (15)$$

Shannon information entropy for the Newcomb–Benford distribution can also be computed when addressing the dataset at the fifth column of Table II, yielding

$$S_{\text{BENF}} = - \sum_{d=1}^9 P_{\text{BENF}}(d) \ln P_{\text{BENF}}(d) \approx 1.996 \text{ nat.} \quad (16)$$

The Shannon information entropy deficit reads

$$\Delta S = S_{\text{BENF}} - S_{\text{OBS}} \approx 0.524 \text{ nat,} \quad (17)$$

encoding a 26.25% Shannon information entropy deficit coming from scale invariance breaking due to QCD dynamics. From a purely statistical viewpoint, Newcomb–Benford’s law corresponds to the maximum-Shannon information entropy distribution of leading digits under scale invariance, where all logarithmic decades are equally probable, and no physical scale dominates. However, the leading-digit distribution of the baryon mass spectrum in PDG reveals a Shannon information entropy deficit (17), meaning that the digit distribution carries measurable information about the emergence of Λ_{QCD} . The χ^2 test yields $\chi^2_{\text{OBS}} = 124.320$, with p -value given by $p = P(\chi^2 \geq 124.320) \lesssim 4.241 \times 10^{-23}$, which is extremely small, indicating a very significant deviation from the expected Newcomb–Benford distribution.

C. Shannon information entropy for mesons (with further mesonic states) and baryons in PDG

The leading-digit statistics of meson and baryon mass spectra will be investigated. Table III reports the observed and expected frequencies, together with the probabilities from Newcomb–Benford’s law for $N = 525$ entries.

Digit (d)	Observed (\mathcal{O}_d)	$P_{\text{OBS}}(d)$	Benford (\mathcal{E}_d)	$P_{\text{BENF}}(d)$
1	176	0.335	113.2	0.301
2	197	0.375	66.2	0.176
3	45	0.086	47.0	0.125
4	41	0.078	36.5	0.097
5	26	0.050	29.7	0.079
6	24	0.046	25.2	0.067
7	3	0.006	21.8	0.058
8	1	0.002	19.2	0.051
9	12	0.023	17.3	0.046

TABLE III Comparison of the leading-digit distribution of meson (with further mesonic states) and baryon masses in PDG to the Newcomb–Benford’s probability distribution ($N = 525$).

Fig. 5 depicts the observed hadronic mass spectrum.

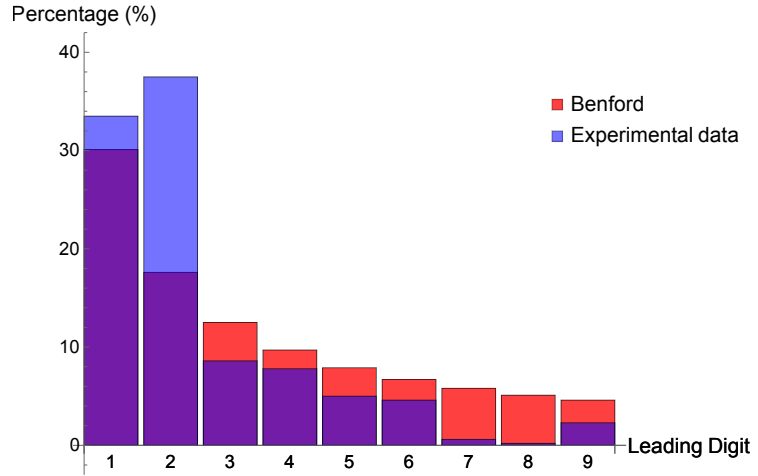


FIG. 5 Distribution of the meson mass spectrum with further mesonic states and baryons in PDG [21], according to the leading digit.

Digits 1 and 2 are overrepresented, while higher numbers are underrepresented relative to the ideal logarithmic Newcomb–Benford distribution, although clustering is again observed in the leading digit 9. Shannon information entropy of the observed baryon mass

spectrum can be calculated by the third column of Table III, yielding

$$S_{\text{PDG}} = - \sum_{d=1}^9 P_{\text{OBS}}(d) \ln P_{\text{OBS}}(d) \approx 1.566 \text{ nat.} \quad (18)$$

The Shannon information entropy for the Newcomb–Benford distribution can be computed when addressing the dataset at the fifth column of Table III, yielding

$$S_{\text{BENF}} = - \sum_{d=1}^9 P_{\text{BENF}}(d) \ln P_{\text{BENF}}(d) \approx 1.996 \text{ nat}, \quad (19)$$

implying the Shannon information entropy deficit:

$$\Delta S = S_{\text{BENF}} - S_{\text{OBS}} \approx 0.430 \text{ nat}, \quad (20)$$

representing a 21.55% reduction. Analogously to what has been reported for baryons and mesons separately in the previous subsections, the combined mesonic and baryonic mass spectra show that $\chi_{\text{OBS}}^2 = 329.525$. The p -value $p = P(\chi^2 \geq 329.525) \lesssim 2.110 \times 10^{-66}$ is infinitesimal, showing that the leading-digit distribution of the hadronic mass spectrum drastically deviates from the expected Newcomb–Benford distribution. The deviation is primarily due to the overpopulation of digits 1 and 2. The Shannon information entropy deficit (20) quantifies the information gained from QCD dynamical emergence of the scale Λ_{QCD} . Thus, the combined meson and baryon leading-digit statistics transform deviations from the law of anomalous numbers into an information-theoretic indication of the QCD scale. The hadronic mass spectrum clusters around certain mass ranges, suppressing the logarithmic uniformity in the hadronic mass leading digit.

IV. CONCLUDING REMARKS

The analysis of the leading-digit distribution of hadron masses imprints a clear signature of scale-invariance breaking in QCD into the information entropy. When compared with Newcomb–Benford’s law, the leading-digit distribution of hadronic masses in PDG systematically deviates from the logarithmic pattern expected in a scale-free theory. In each case here studied, the Shannon information entropy quantifies this deviation, and its deficit represents the information cost of scale generation in QCD. The observed reduction in Shannon information entropy thus encodes the emergence of Λ_{QCD} as an intrinsic source of scale, via dimensional transmutation, into a quantized hierarchy of mass gaps between hadronic mass clusters. The leading-digit distribution of the hadronic mass spectrum can therefore be regarded as information entropy reduction driven by the dynamical

breaking of scale invariance in QCD. Shannon information entropy deficits can measure how much less random the hadronic mass distribution becomes when quantum corrections introduce a preferred energy scale, leaving an imprint of QCD dynamics within the statistical organization of the hadronic mass spectrum.

For the distribution of the mesons mass spectrum, the Shannon information entropy deficit $\Delta S \approx 0.427$ nat represents a 21.37% deviation from the log-uniform distribution, measuring the anomalous breaking of scale symmetry in QCD, as a byproduct of enhanced clustering around relevant mass ranges. The leading-digit distribution of the baryonic mass spectrum shows an even stronger deficit, $\Delta S \approx 0.524$ nat (26.25%). When mesons and baryons are analyzed together, the deficit stabilizes at $\Delta S \approx 0.430$ nat (21.55%), confirming a robust information-theoretic imprint of anomalous breaking of scale symmetry in QCD across the entire hadronic mass spectrum in PDG [21]. In a scale-invariant regime, as implied by Newcomb–Benford statistics, Shannon information entropy would be maximal ($S_{\text{BENF}} \approx 1.996$ nat). The χ^2 tests corroborate these findings. In all three datasets containing mesons and baryons, the χ^2_{OBS} values reach astronomically small p -values ($10^{-23} \lesssim p \lesssim 10^{-66}$). It decisively suppresses the null hypothesis that hadronic mass spectra follow Newcomb–Benford’s law, which encodes QCD-preferred energy scales rather than logarithmic uniformity typical of scale-invariant systems. Thus, Shannon information entropy of the hadronic mass spectrum provides a quantitative, model-independent measure of anomalous breaking of scale symmetry in QCD.

Acknowledgments: RdR thanks The São Paulo Research Foundation – FAPESP (Grants No. 2021/01089-1 and No. 2024/05676-7), and the National Council for Scientific and Technological Development – CNPq (Grants No. 303742/2023-2 and No. 401567/2023-0), for partial financial support. RDV warmly thanks E. Gueron for introducing him to Newcomb–Benford statistics and for enlightening discussions.

Appendix A: Newcomb–Benford’s law as the maximum Shannon information entropy distribution under scale invariance: A variational principle derivation

We want to obtain the probability density $P(x)$ on the real interval $[x_{\text{MIN}}, x_{\text{MAX}}]$ that maximizes Shannon information entropy

$$S[P] = - \int_{x_{\text{MIN}}}^{x_{\text{MAX}}} P(x) \ln P(x) dx, \quad (\text{A1})$$

with normalization

$$\int_{x_{\text{MIN}}}^{x_{\text{MAX}}} P(x) dx = 1, \quad (\text{A2})$$

and scale invariance $P(\lambda x) = \frac{1}{\lambda} P(x)$, $\lambda \in \mathbb{R}^+$. Differentiating with respect to λ and evaluating at $\lambda = 1$ gives the infinitesimal constraint

$$x P'(x) + P(x) = 0. \quad (\text{A3})$$

The variational problem can be posed by extremizing $S[P]$ with the two constraints (A2) and (A3). One can introduce a Lagrange multiplier λ for normalization and a local multiplier $\mu(x)$ for the infinitesimal constraint. The augmented functional can be written as

$$\mathcal{L}[P] = - \int_{x_{\text{MIN}}}^{x_{\text{MAX}}} P(x) \ln P(x) dx + \lambda \left(\int_{x_{\text{MIN}}}^{x_{\text{MAX}}} P(x) dx - 1 \right) + \int_{x_{\text{MIN}}}^{x_{\text{MAX}}} \mu(x) [x P'(x) + P(x)] dx. \quad (\text{A4})$$

Integrating by parts and assuming the boundary term vanishes, the first variation reads

$$\delta \mathcal{L} = \int_{x_{\text{MIN}}}^{x_{\text{MAX}}} \delta P(x) \left[-\ln P + 1 + \lambda - x \mu'(x) \right] dx = 0, \quad (\text{A5})$$

implying that

$$\ln P(x) = \lambda - 1 - x \mu'(x). \quad (\text{A6})$$

Differentiating Eq. (A6) gives $\frac{P'(x)}{P(x)} = -\mu'(x) - x \mu''(x)$. Using the constraint (A3), one obtains

$$x \mu''(x) + \mu'(x) = \frac{1}{x}. \quad (\text{A7})$$

Let $\xi(x) \equiv \mu'(x)$. Then $(x \xi)' = 1/x$, which integrates to

$$x \mu'(x) = \ln x + c_1, \quad (\text{A8})$$

$$\mu(x) = \frac{1}{2} (\ln x)^2 + c_1 \ln x + c_2, \quad (\text{A9})$$

for c_1, c_2 constants. Substituting Eq. (A8) into Eq. (A6) yields

$$\ln P(x) = (\lambda - 1 - c_1) - \ln x, \quad \Rightarrow \quad P(x) = A x^{-1}. \quad (\text{A10})$$

Normalization gives

$$1 = \int_{x_{\text{MIN}}}^{x_{\text{MAX}}} A \frac{dx}{x} = A \ln \left(\frac{x_{\text{MAX}}}{x_{\text{MIN}}} \right) \quad \Rightarrow \quad A = \frac{1}{\ln(x_{\text{MAX}}/x_{\text{MIN}})}. \quad (\text{A11})$$

Hence, the maximum-Shannon information entropy, scale-invariant probability density reads

$$P(x) = \frac{1}{x \ln(x_{\text{MAX}}/x_{\text{MIN}})}, \quad x \in [x_{\text{MIN}}, x_{\text{MAX}}]. \quad (\text{A12})$$

The corresponding Shannon information entropy is given by

$$S_{\text{MAX}} = - \int_{x_{\text{MIN}}}^{x_{\text{MAX}}} \frac{1}{x \ln\left(\frac{x_{\text{MAX}}}{x_{\text{MIN}}}\right)} \ln\left(\frac{1}{x \ln\left(\frac{x_{\text{MAX}}}{x_{\text{MIN}}}\right)}\right) dx, \quad (\text{A13})$$

which simplifies to

$$\begin{aligned} S_{\text{MAX}} &= \frac{1}{\ln\left(\frac{x_{\text{MAX}}}{x_{\text{MIN}}}\right)} \left[\frac{1}{2} (\ln^2 x_{\text{MAX}} - \ln^2 x_{\text{MIN}}) + \ln \ln\left(\frac{x_{\text{MAX}}}{x_{\text{MIN}}}\right) (\ln x_{\text{MAX}} - \ln x_{\text{MIN}}) \right] \\ &= \ln \left[\ln\left(\frac{x_{\text{MAX}}}{x_{\text{MIN}}}\right) \sqrt{x_{\text{MAX}} x_{\text{MIN}}} \right]. \end{aligned} \quad (\text{A14})$$

Thus, the Shannon information entropy grows logarithmically with the multiplicative range $\ln(x_{\text{MAX}}/x_{\text{MIN}})$, reflecting scale invariance.

Appendix B: Anomalous breaking of scale symmetry in QCD, the mass gap, and hadron density of states

For N_f massless quark flavors, the classical QCD Lagrangian is given by

$$\mathcal{L}_{\text{QCD}} = -\frac{1}{4} G_{\mu\nu}^a G^{\mu\nu a} + i\hbar \bar{\psi} \gamma^\mu D_\mu \psi, \quad (\text{B1})$$

for the gluon field strength tensor $G_{\mu\nu}^a = \partial_{[\mu} A_{\nu]}^a + g_s f^{abc} A_\mu^b A_\nu^c$ and the covariant derivative $D_\mu = \partial_\mu - ig_s T^a A_\mu^a$. The coupling g_s governs quark–gluon and gluon–gluon interactions and represents the gauge coupling constant of the color group $\text{SU}(N_c)$ [37, 38], for N_c denoting the numbers of colors, and T^a the special unitary group generators satisfying $[T^a, T^b] = if^{abc} T^c$ and $\text{Tr}(T^a T^b) = \frac{1}{2} \delta^{ab}$, with f^{abc} the structure constants.

For vanishing quark masses, the action (B1) is also invariant under the global chiral symmetry $\text{SU}(N_f)_L \times \text{SU}(N_f)_R$, with the corresponding mappings $\psi_{L,R} \mapsto U_{L,R} \psi_{L,R}$. The classical action is furthermore invariant under the scale transformations

$$x^\mu \mapsto \lambda x^\mu, \quad A_\mu(x) \mapsto \lambda^{-1} A_\mu(\lambda^{-1} x), \quad \psi(x) \mapsto \lambda^{-3/2} \psi(\lambda^{-1} x), \quad (\text{B2})$$

so that *classical* QCD is both chiral and scale invariant. The Noether dilatation current $D^\mu = x_\nu T^{\mu\nu}$ has divergence $\partial_\mu D^\mu = T^\mu_\mu$. Hence, scale invariance implies $T^\mu_\mu = 0$. A nonzero trace indicates a breaking of scale symmetry, resulting in the trace anomaly. At the quantum level, renormalization introduces a dimensionful scale μ , and the coupling becomes scale-dependent,

$$\mu \frac{dg_s}{d\mu} = \beta(g_s) = -\frac{g_s^3}{16\pi^2} \left(11 - \frac{2}{3} N_f \right). \quad (\text{B3})$$

The nonvanishing β -function breaks scale invariance and defines the QCD scale Λ_{QCD} through dimensional transmutation. Solving the renormalization-group equation (B3) at one loop gives the standard expression for the running coupling,

$$\alpha_s(\mu) = \frac{4\pi}{(11 - \frac{2}{3}N_f) \ln(\mu^2/\Lambda_{\text{QCD}}^2)}, \quad (\text{B4})$$

where $\alpha_s(\mu) \equiv g_s^2(\mu)/4\pi$ stands for the strong coupling constant expressed in terms of the renormalized QCD gauge coupling $g_s(\mu)$ at the scale μ . As $\mu \rightarrow \Lambda_{\text{QCD}}$, the denominator in Eq. (B4) vanishes and $\alpha_s(\mu)$ diverges, signaling confinement. The strong coupling becomes of order unity, implying that the perturbative expansion in powers of g_s ceases to be reliable. In this regime, the short-distance degrees of freedom (quarks and gluons) can no longer be treated as weakly interacting. Lattice QCD yields the value $\alpha_s(M_Z) = 0.1179 \pm 0.0010$, where the Z boson mass is given by $M_Z = 91.1876 \pm 0.0021$ GeV [21, 42].

The corresponding trace anomaly reads

$$T^\mu_\mu = \frac{\beta(g_s)}{2g_s} G_{\mu\nu}^a G^{\mu\nu a} + (1 + \gamma_m) \sum_f m_f \bar{\psi}_f \psi_f, \quad (\text{B5})$$

with $\gamma_m(g_s)$ denoting the anomalous dimension of the quark mass operator. At leading order in QCD, it reads

$$\gamma_m(g_s) = \frac{3(N_c^2 - 1)}{32\pi^2 N_c} g_s^2 + \mathcal{O}(g_s^4), \quad (\text{B6})$$

accounting for the quantum correction to the scaling dimension in the term $m_f \bar{\psi}_f \psi_f$. Quantum effects make the dimensionful scale $\Lambda_{\text{QCD}} \sim 200\text{-}300$ MeV emerge.

Ordinary mesons, as $q\bar{q}$ bound states, satisfy $M_{q\bar{q}} \neq m_q + m_{\bar{q}}$, since most of their mass originates from confinement and QCD binding energy. Although the light-quark QCD Lagrangian is nearly scale invariant, quantum corrections generate the scale Λ_{QCD} , which determines hadronic masses. In the massless quark limit, the (pseudo-)Goldstone bosons π , K , and η , have small masses arising from chiral symmetry breaking. Vector mesons such as $\rho(770)$, $\omega(782)$, $K^*(892)$, and $\phi(1020)$ cluster around $0.8 \sim 1.0$ GeV, with a mass gap around 0.6 GeV reflecting hyperfine splitting. Higher hadron excitations follow Regge trajectories relating the angular momentum J and the meson mass M , as $J \propto \alpha' M^2$, where $\alpha' \approx (2\pi\sigma)^{-1} \approx 0.9$ GeV $^{-2}$, with σ the string tension [43]. For heavy quarks, $m_Q \gg \Lambda_{\text{QCD}}$, meson masses are dominated by the term $2m_Q$, while level spacings remain at the order of Λ_{QCD} . Quarkonia exhibit radial splittings of 0.5 GeV ~ 0.6 GeV. This universal spacing reflects confinement rather than the quark masses themselves.

Empirically, the hadron density of states grows exponentially with mass, $\rho(M) \propto e^{M/T_{\text{H}}}$ in the statistical bootstrap model, with $T_{\text{H}} \simeq 150\text{-}180$ MeV being the Hagedorn

temperature [44]. It arises from the combinatorics of string-like excitations of confined flux tubes [45]. The number of hadron states below a given mass M then satisfies

$$N(M) = \int_0^M \rho(M') dM', \quad (\text{B7})$$

which approximately doubles with every ~ 150 MeV increase in M . The deconfinement temperature range $121 \text{ MeV} \lesssim T_{\text{H}} \lesssim 171 \text{ MeV}$ was derived in both holographic and lattice QCD [46], while the interval $191 \text{ MeV} \lesssim T_{\text{H}} \lesssim 202 \text{ MeV}$ regards AdS/QCD models. The glueball spectrum yields $T_{\text{H}} \approx 175.4 \pm 15.2 \text{ MeV}$ [47–49], the HotQCD Collaboration obtained the critical deconfinement temperature $T_c = 156.5 \pm 1.5 \text{ MeV}$ [50], and the Wuppertal–Budapest Collaboration yielded $T_c = 158.0 \pm 0.6 \text{ MeV}$ [51]. Holographic entanglement entropy in AdS/QCD supports these last results [52–54].

The canonical partition function of the hadronic spectrum can be written as

$$Z(T) = \int_{M_{\text{GAP}}}^{\infty} \rho(M) e^{-M/T} dM, \quad (\text{B8})$$

The mass gap prevents the existence of hadronic states of arbitrarily small nonzero mass. In fact, denoting by M_{GAP} the lowest allowed mass, one has $M_{\text{GAP}} = M_{\pi}$, if $m_q \neq 0$, or $M_{\text{GAP}} \sim \Lambda_{\text{QCD}}$, in pure Yang-Mills theory. At high masses, writing a more precise form for the Hagedorn density of states, $\rho(M) \propto M^{-a} e^{M/T_{\text{H}}}$, makes the integrand in Eq. (B8) behave as $M^{-a} e^{-M(1/T-1/T_{\text{H}})}$. Hence $Z(T)$ converges for $T < T_{\text{H}}$ and diverges for $T \geq T_{\text{H}}$ (for typical $a \sim 5/2$ in Hagedorn’s original model), indicating that added energy near T_{H} produces new hadronic resonances rather than raising temperature, pointing to deconfinement transition to QGP [55, 56]. The exponential growth of the density of states $\rho(M)$ thus defines the Hagedorn temperature as the limiting point of the canonical ensemble, linking the low-energy mass gap to the high-energy onset of deconfinement [57]. A relativistic string with tension σ exhibits mass spectrum $M_n^2 \sim \sigma n$ [58] and $T_{\text{H}} \propto \sqrt{\sigma}$. The cumulative distribution $\ln N(M) \approx M/T_{\text{H}}$ demonstrates the exponential Hagedorn behavior. Confinement corresponds to finite-energy flux tubes with tension $\sigma \sim \Lambda_{\text{QCD}}^2$, whose quantized vibrations generate the hadron tower. Thus, the mass gap (infrared confinement) and Hagedorn growth (ultraviolet spectrum) are dual manifestations of the same QCD scale.

[1] C. E. Shannon, The Bell System Technical Journal **27**, 379 (1948).

- [2] G. Karapetyan, Phys. Lett. B **781**, 201 (2018), 1802.09105.
- [3] G. Karapetyan, Annals Phys. **462**, 169612 (2024), 2305.05413.
- [4] C.-W. Ma and Y.-G. Ma, Prog. Part. Nucl. Phys. **99**, 120 (2018), 1801.02192.
- [5] M. Gleiser, M. Stephens, and D. Sowinski, Phys. Rev. D **97**, 096007 (2018), 1803.08550.
- [6] M. Gleiser and D. Sowinski, Phys. Rev. D **98**, 056026 (2018), 1807.07588.
- [7] A. E. Bernardini and R. da Rocha, Phys. Lett. B **762**, 107 (2016), 1605.00294.
- [8] E. Witten, Riv. Nuovo Cim. **43**, 187 (2020), 1805.11965.
- [9] A. E. Bernardini and R. da Rocha, Phys. Rev. D **98**, 126011 (2018), 1809.10055.
- [10] G. Karapetyan, Phys. Lett. B **786**, 418 (2018), 1807.04540.
- [11] M. A. Martin Contreras and A. Vega, Phys. Rev. D **102**, 046007 (2020), 2004.10286.
- [12] N. R. F. Braga, L. F. Faulhaber, and O. C. Junqueira, Phys. Rev. D **105**, 106003 (2022), 2201.05581.
- [13] R. da Rocha and P. H. O. Silva, Phys. Rev. D **110**, 126019 (2024), 2412.02375.
- [14] L. F. Ferreira and R. da Rocha, Phys. Rev. D **99**, 086001 (2019), 1902.04534.
- [15] P. Colangelo and F. Loparco, Phys. Lett. B **788**, 500 (2019), 1811.05272.
- [16] C.-W. Ma, H.-L. Wei, S.-S. Wang, Y.-G. Ma, R. Wada, and Y.-L. Zhang, Phys. Lett. B **742**, 19 (2015).
- [17] M. A. Martin Contreras and A. Vega, Phys. Rev. D **108**, 126024 (2023), 2309.02905.
- [18] L. F. Ferreira and R. da Rocha, Phys. Rev. D **101**, 106002 (2020), 2004.04551.
- [19] M. A. Martin Contreras, A. Vega, and S. Diles, Phys. Lett. B **835**, 137551 (2022), 2206.01834.
- [20] X. Guo, M. A. Martin Contreras, X. Chen, and D. Xiang, Chin. Phys. C **49**, 013104 (2025), 2404.16608.
- [21] S. Navas et al. (Particle Data Group), Phys. Rev. D **110**, 030001 (2024).
- [22] R. A. C. Correa, R. da Rocha, and A. de Souza Dutra, Annals Phys. **359**, 198 (2015), 1501.02000.
- [23] M. Gleiser and N. Stamatopoulos, Phys. Rev. D **86**, 045004 (2012), 1205.3061.
- [24] D. Bazeia and E. I. B. Rodrigues, Phys. Lett. A **392**, 127170 (2021), 2206.06351.
- [25] Y. Mvondo-She, JHEP **03**, 192 (2023), 2302.07331.
- [26] R. Casadio, R. da Rocha, P. Meert, L. Tabaroni, and W. Barreto, Class. Quant. Grav. **40**, 075014 (2023), 2206.10398.
- [27] L. Shao and B.-Q. Ma, Mod. Phys. Lett. A **24**, 3275 (2009), 1004.3077.

- [28] F. Benford, Proc. Am. Philos. Soc. **78**, 551 (1938).
- [29] H. Jiang, J.-J. Shen, and Y.-M. Zhao, Chin. Phys. Lett. **28**, 032101 (2011).
- [30] L. Shao and B.-Q. Ma, Astropart. Phys. **33**, 255 (2010), 1005.1702.
- [31] H.-Y. Lai and J.-J. Wei, Res. Astron. Astrophys. **24**, 055007 (2024), 2401.10609.
- [32] A. Bera, U. Mishra, S. S. Roy, A. Biswas, A. S. De, and U. Sen, Phys. Lett. A **382**, 1639 (2018), 1711.00758.
- [33] L. Shao and B.-Q. Ma, Physica A **389**, 3109 (2010), 1005.0660.
- [34] R. Hagedorn, Nuovo Cim. Suppl. **6**, 311 (1968).
- [35] K. G. Wilson, Phys. Rev. B **4**, 3174 (1971).
- [36] J. Polchinski, Nucl. Phys. B **231**, 269 (1984).
- [37] D. J. Gross and F. Wilczek, Phys. Rev. Lett. **30**, 1343 (1973).
- [38] H. D. Politzer, Phys. Rev. Lett. **30**, 1346 (1973).
- [39] D. C. Duarte, T. Frederico, W. de Paula, and E. Ydrefors, Phys. Rev. D **105**, 114055 (2022), 2204.08091.
- [40] G. Torrieri and J. Noronha, Phys. Lett. B **690**, 477 (2010), 1004.0237.
- [41] C. E. Fontoura, G. Krein, A. Valcarce, and J. Vijande, Phys. Rev. D **112**, 014007 (2025), 2506.07090.
- [42] A. Bazavov, N. Brambilla, X. Garcia i Tormo, P. Petreczky, J. Soto, A. Vairo, and J. H. Weber (TUMQCD), Phys. Rev. D **100**, 114511 (2019), 1907.11747.
- [43] T. Regge, Nuovo Cim. **14**, 951 (1959).
- [44] R. Hagedorn, Nuovo Cim. A **56**, 1027 (1968).
- [45] N. Isgur and J. E. Paton, Phys. Rev. D **31**, 2910 (1985).
- [46] A. Cucchieri and T. Mendes, Phys. Rev. Lett. **100**, 241601 (2008), 0712.3517.
- [47] S. S. Afonin and A. D. Katanaeva, Phys. Rev. D **98**, 114027 (2018), 1809.07730.
- [48] D. Dудal and S. Mahapatra, Phys. Rev. D **96**, 126010 (2017), 1708.06995.
- [49] N. R. F. Braga and O. C. Junqueira, Phys. Lett. B **814**, 136082 (2021), 2010.00714.
- [50] A. Bazavov et al. (HotQCD), Phys. Lett. B **795**, 15 (2019), 1812.08235.
- [51] S. Borsanyi, Z. Fodor, J. N. Guenther, R. Kara, S. D. Katz, P. Parotto, A. Pasztor, C. Ratti, and K. K. Szabo, Phys. Rev. Lett. **125**, 052001 (2020), 2002.02821.
- [52] R. da Rocha, Eur. Phys. J. Plus **139**, 1006 (2024), 2409.17325.
- [53] J. Ovalle, R. Casadio, R. da Rocha, A. Sotomayor, and Z. Stuchlik, EPL **124**, 20004 (2018), 1811.08559.

- [54] B. Toniato, D. Dudal, S. Mahapatra, R. da Rocha, and S. S. Jena, Phys. Rev. D **111**, 126021 (2025), 2502.12694.
- [55] J. Noronha-Hostler, J. Noronha, and C. Greiner, Phys. Rev. Lett. **103**, 172302 (2009), 0811.1571.
- [56] A. Bazavov et al. (HotQCD), Phys. Rev. D **90**, 094503 (2014), 1407.6387.
- [57] F. Karsch, K. Redlich, and A. Tawfik, Phys. Lett. B **571**, 67 (2003), hep-ph/0306208.
- [58] J. F. Arvis, Phys. Lett. B **127**, 106 (1983).